

Supplementary information

Atmospheric Pressure Field Effect Ionisation Source for Ion Mobility Spectrometry

Contents	Page
Figure S1. Graphical abstract.	S2
Figure S2. a) The SEM photograph, b) The electric field simulation at the APFE wire electrode tip.	S2
Figure S3. The electric field simulation at the APCD wire electrode tip.	S3
Table S1. Parameters of APFE ionisation varied in present studies and range of the values.	S4
Figure S4. Negative ion mobility (left) and mass spectra (right) of the dibromo-methane (concentration 240 ppb) the standard gas flow mode a) APFE, b) APCD ionisation sources; the reverse gas flow c) APFE, d) APCD ionisation sources.	S5
Figure S5. Negative ion mobility (left) and mass spectra (right) of the chloroform (concentration 460ppb) the standard gas flow mode a) APFE, b) APCD ionisation sources; the reverse gas flow c) APFE, d) APCD ionisation sources.	S6
Figure S6. Negative ion mobility spectra in standard gas flow of carbon tetrachloride for a) APFE b) APCD ionisation sources and dibromo-methane c) APFE and d) APCD ionisation sources.	S7
Figure S6. Negative ion mobility spectra in reverse gas flow of carbon tetrachloride for a) APFE b) APCD ionisation sources and dibromo-methane c) APFE and d) APCD.	S8
Figure S8. Negative ion mobility spectra of 2,6-dichloroanisole (concentration 216 ppb) in the standard gas flow mode a) APFE, b) APCD ionisation sources and the reverse gas flow mode for c) APFE and d) APCD ionisation sources.	S9
Figure S9. Negative ion mobility spectra of 2,3,5,6-Tetrachloroanisole (concentration 150 ppb) in the standard gas flow mode a) APFE, b) APCD ionisation sources and the reverse gas flow mode for c) APFE and d) APCD ionisation source.	S10

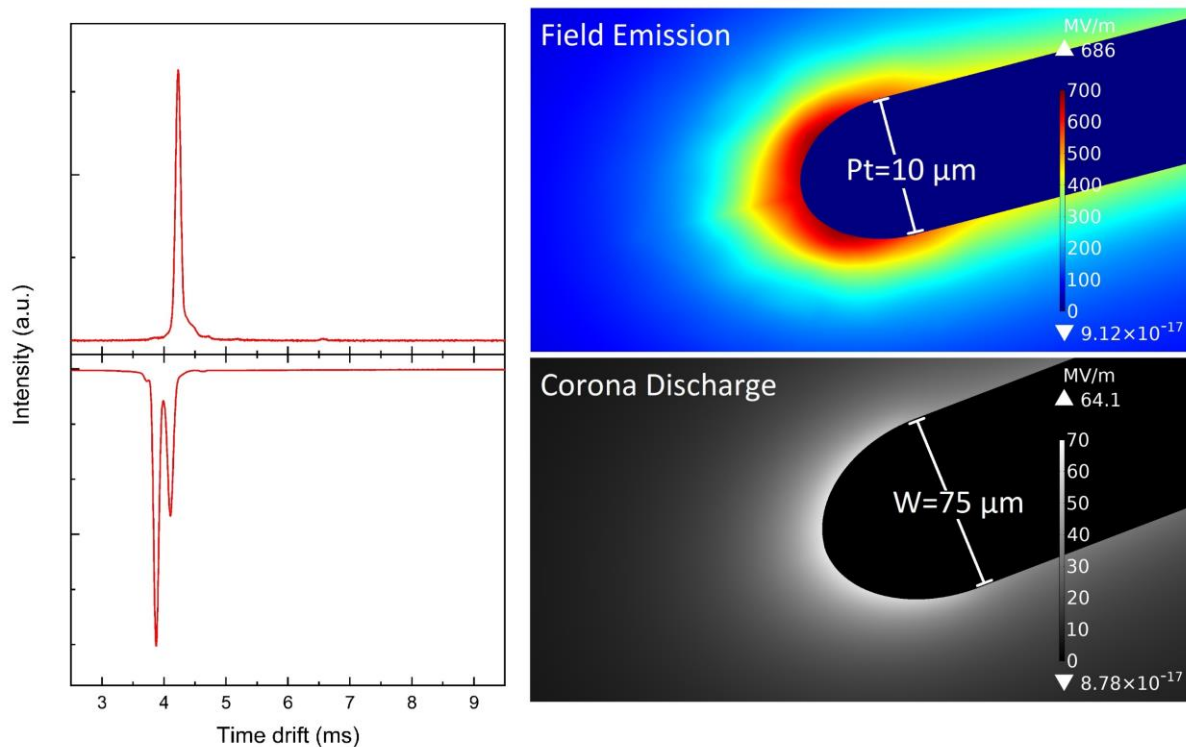


Figure S1. Graphical abstract.

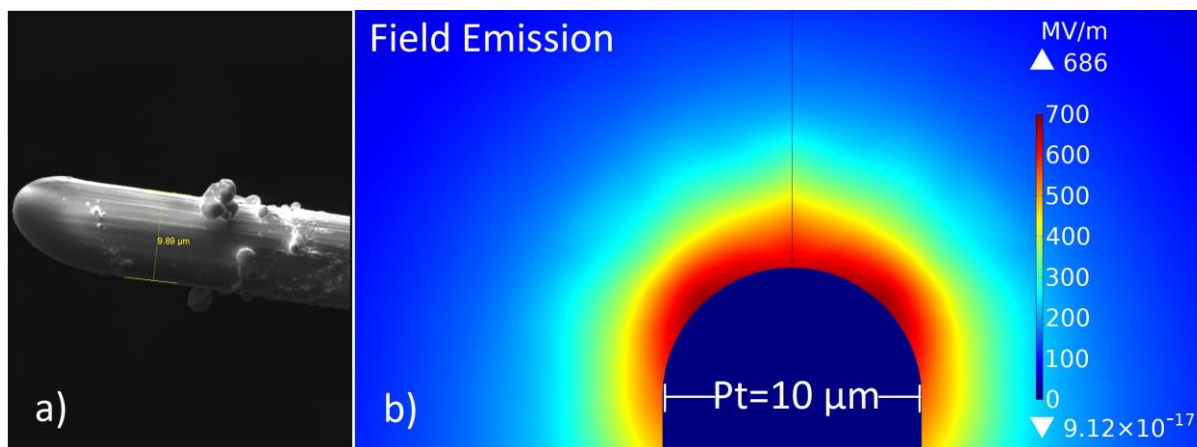


Figure S2. a) The SEM photograph, b) The electric field simulation at the APFE wire electrode tip ($10\ \mu\text{m}$ diameter, $V_1-V_2=9\ \text{kV}$ and $d=12\ \text{mm}$) for the APFE ionisation source.

The simulation has been carried out using the Electrostatics module of COMSOL Multiphysics 3.5a software. The meshing sequences were physics-controlled using extremely fine resolution of element size.

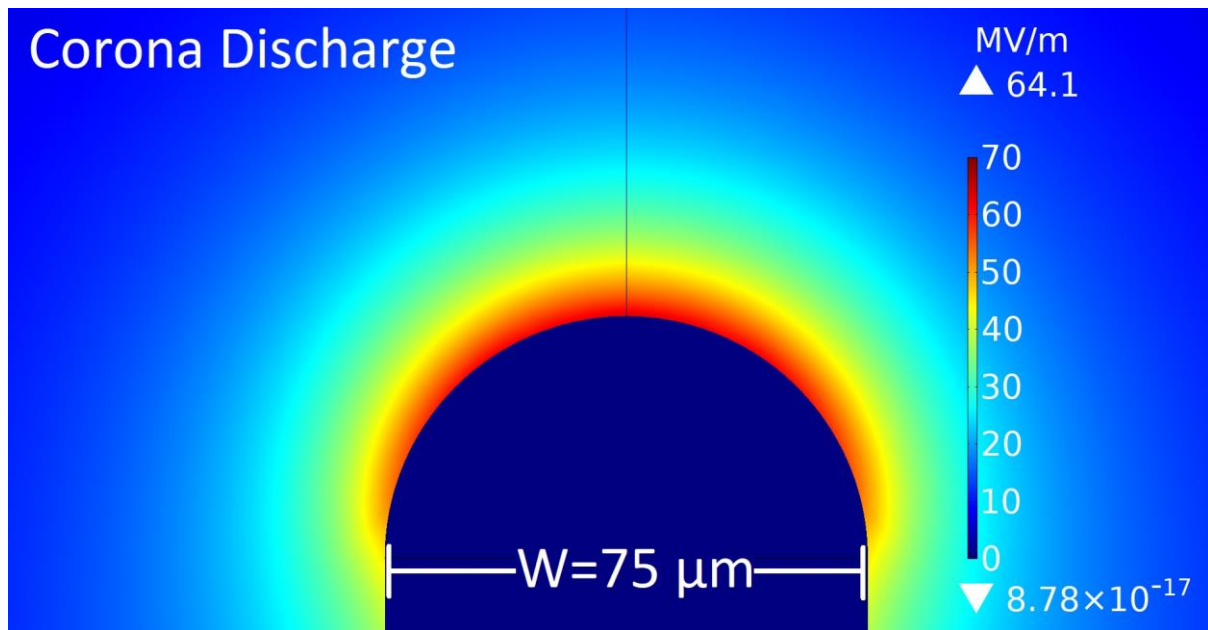


Figure S3. The electric field simulation at the APCD wire electrode tip (75 μm diameter, $V_1-V_2=3.8\ \text{kV}$ and $d=3\ \text{mm}$) for the APCD ionisation source.

The simulation has been carried out using the Electrostatics module of COMSOL Multiphysics 3.5a software. The meshing sequences were physics-controlled using extremely fine resolution of element size.

Table S1. Parameters of APFE ionisation varied in present studies and range of the values.

Wire Material	Wire diameter (μm)	Source stability in positive polarity	Source stability in negative polarity	Lifetime operation in negative polarity	Hole size of plane electrode (mm)	Gap distance (mm)	Resistor value ($\text{G}\Omega$)
tungsten	20	relatively stable	unstable		1-5	1-10	0.5-50
	50	unstable					
	75						
	100						
	Sharp needle (tip diameter= $0.6 \mu\text{m}$)	relatively <i>stable</i>	relatively stable	short lifetime (few hours)			
copper	20	relatively stable			3	1-10	0.5-50
cobalt	20	relatively stable			3	1-10	0.5-50
stainless steel	20	stable			3	1-10	0.5-50
platinum	10	stable	stable	long lifetime	1-5	1-15	0.5-50
	20	stable	relatively stable	short lifetime (few minutes)			
	30	relatively stable	unstable				
gold	20	stable	unstable		4	1-10	0.5-50
	125	relatively stable					
silver	20	relatively stable			4	1-10	0.5-50

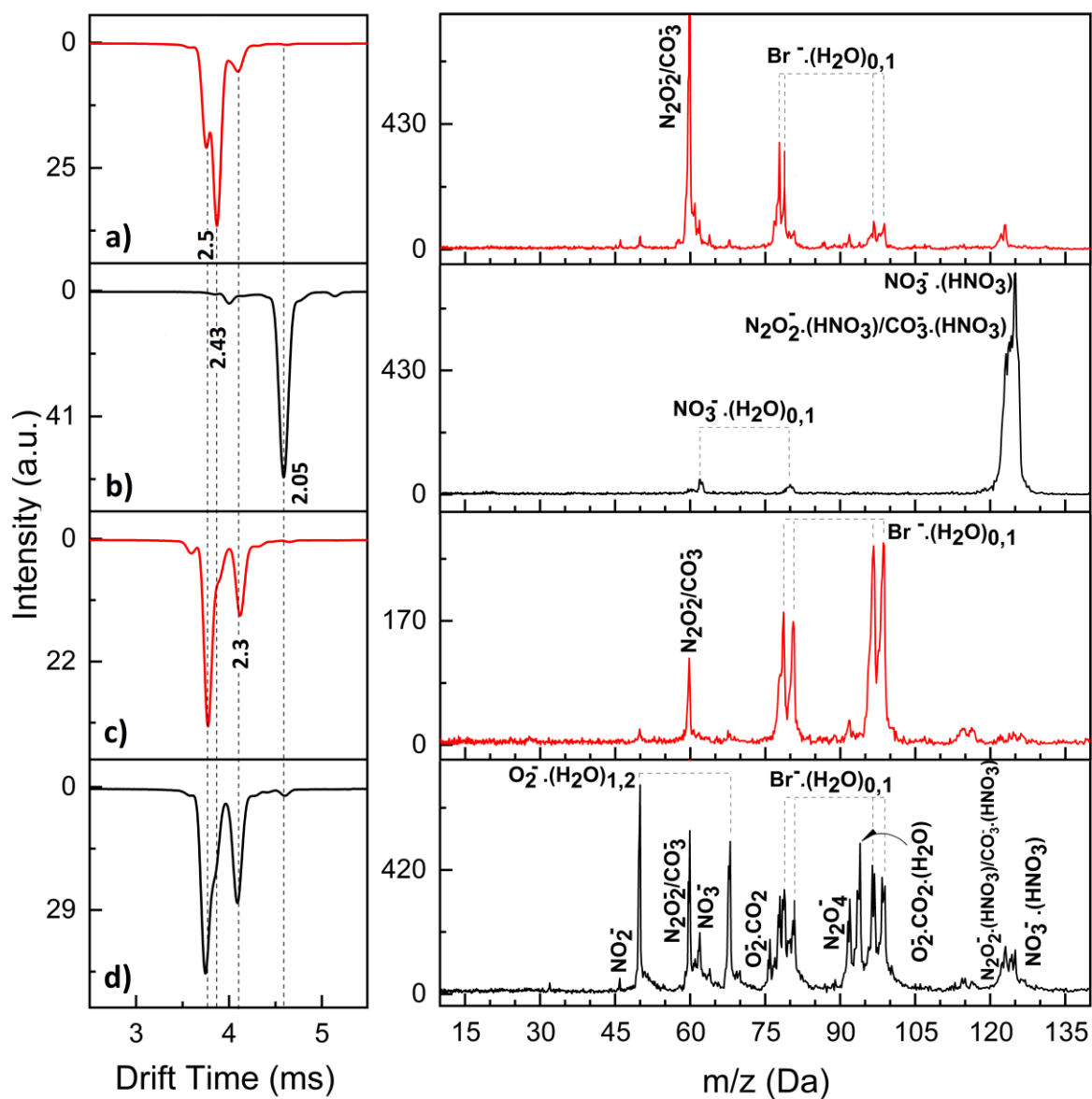


Figure S4. Negative ion mobility (left) and mass spectra (right) of the dibromo-methane (concentration 240 ppb) the standard gas flow mode a) APFE, b) APCD ionisation sources; the reverse gas flow c) APFE, d) APCD ionisation sources.

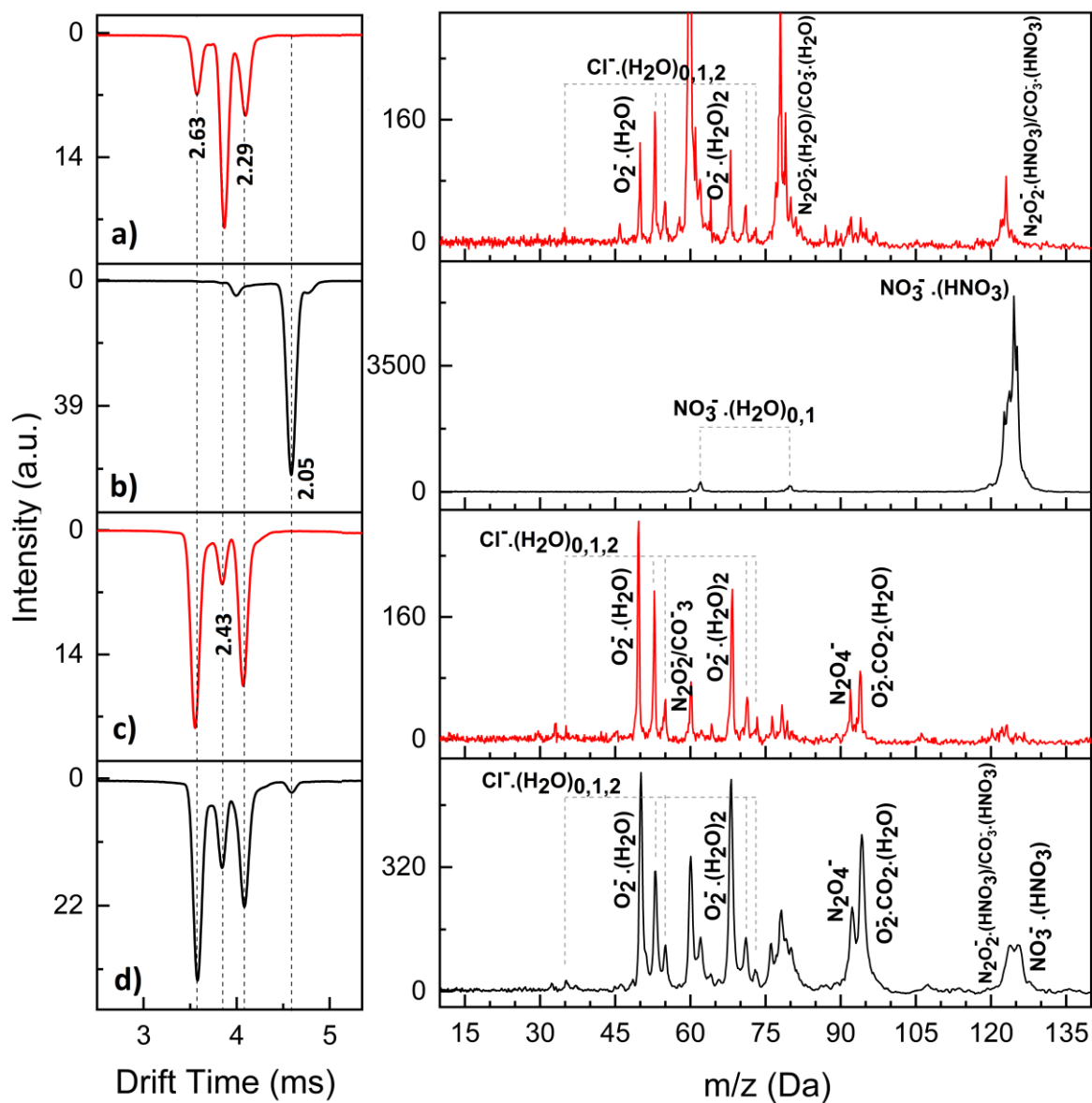


Figure S5. Negative ion mobility (left) and mass spectra (right) of the chloroform (concentration 460ppb) the standard gas flow mode a) APFE, b) APCD ionisation sources; the reverse gas flow c) APFE, d) APCD ionisation sources.

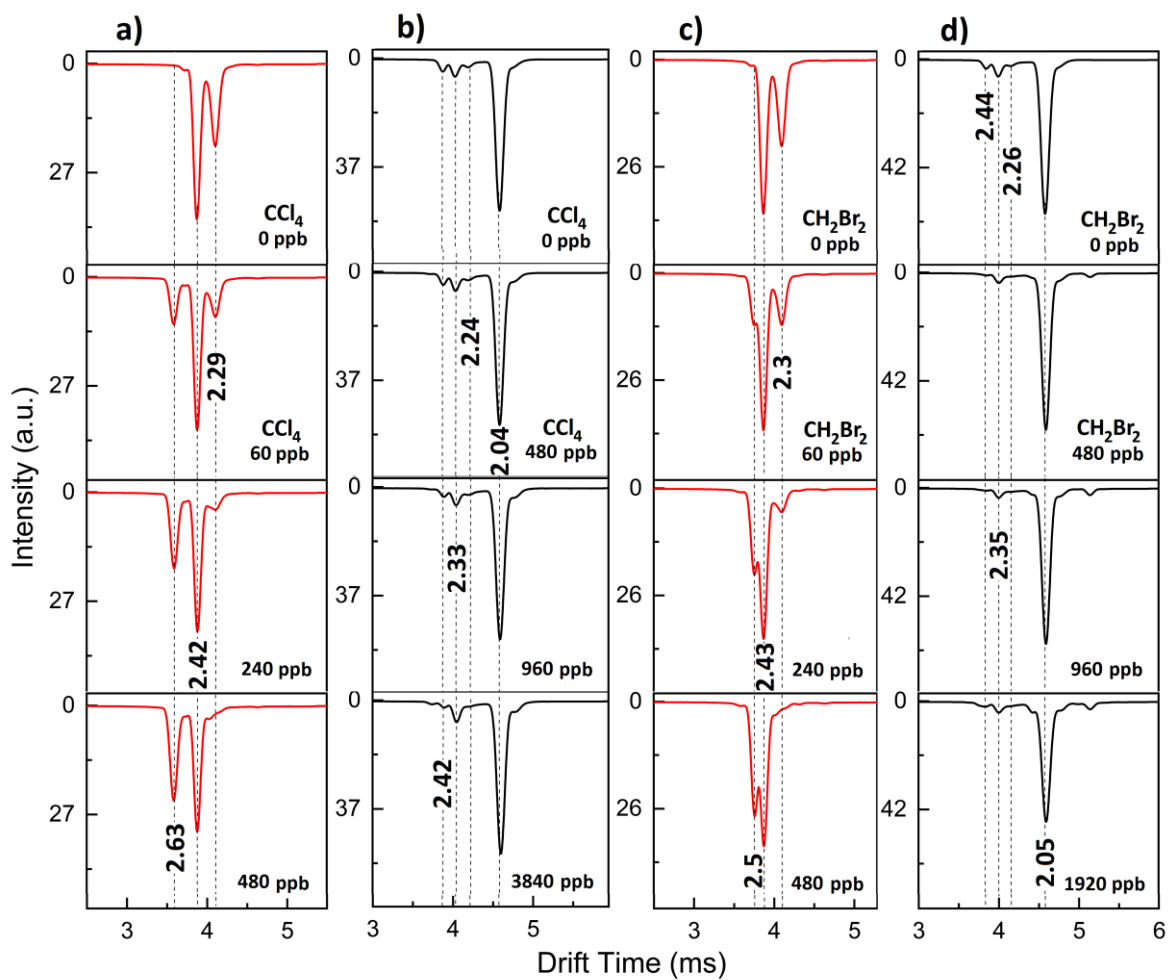


Figure S6. Negative ion mobility spectra in standard gas flow for carbon tetrachloride a) APFE b) APCD ionisation sources and dibromo-methane c) APFE and d) APCD ionisation sources.

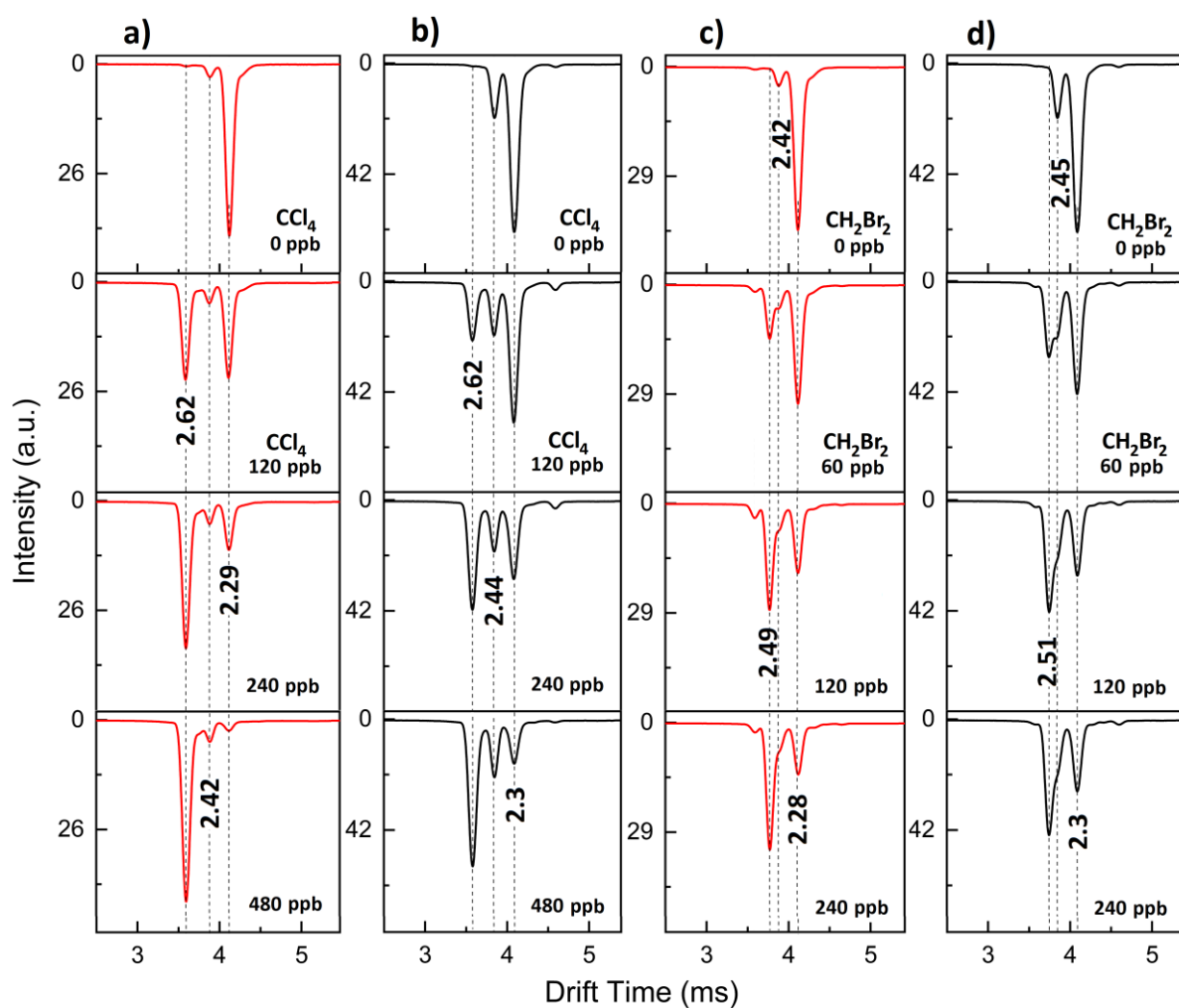


Figure S7. Negative ion mobility spectra in reverse gas flow for carbon tetrachloride a) APFE b) APCD ionisation sources and dibromo-methane c) APFE and d) APCD ionisation sources.

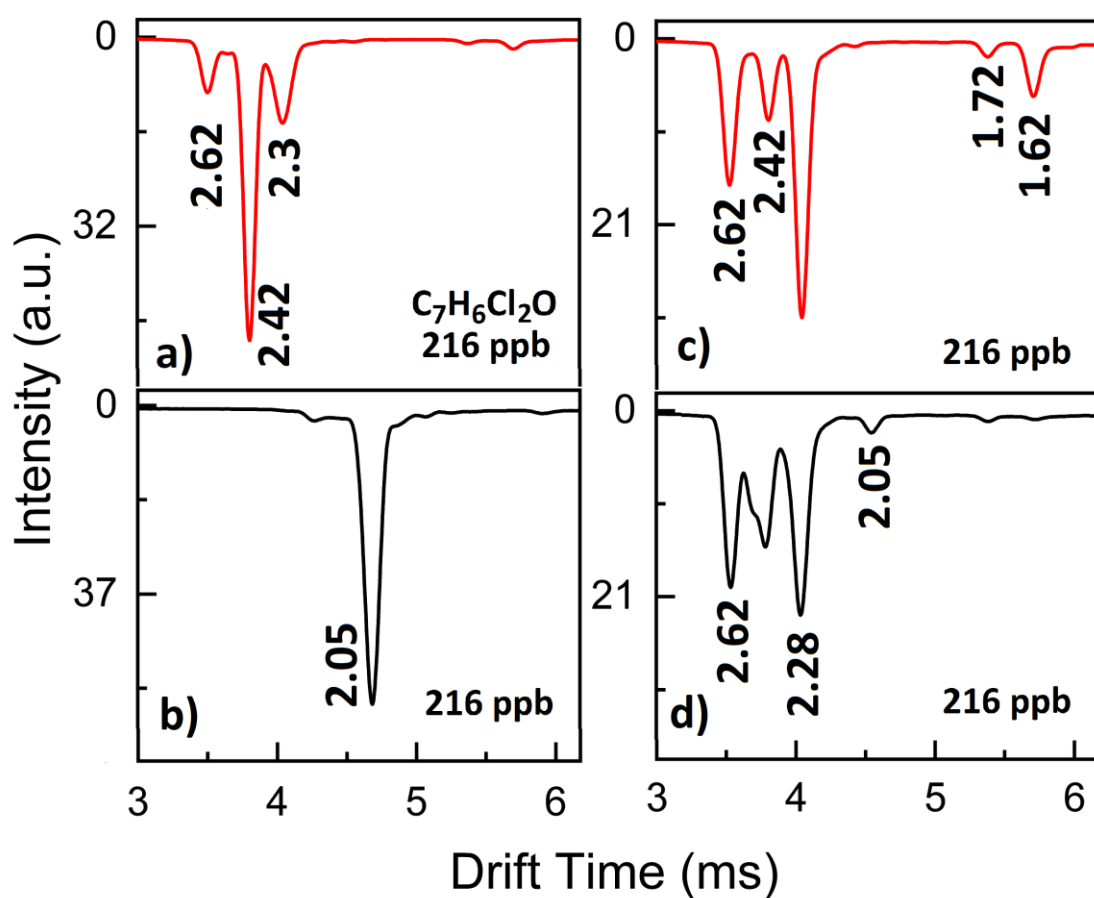


Figure S8. Negative ion mobility spectra of 2,6-dichloroanisole (concentration 216 ppb) in the standard gas flow mode a) APFE, b) APCD ionisation sources and the reverse gas flow mode for c) APFE and d) APCD ionisation sources.

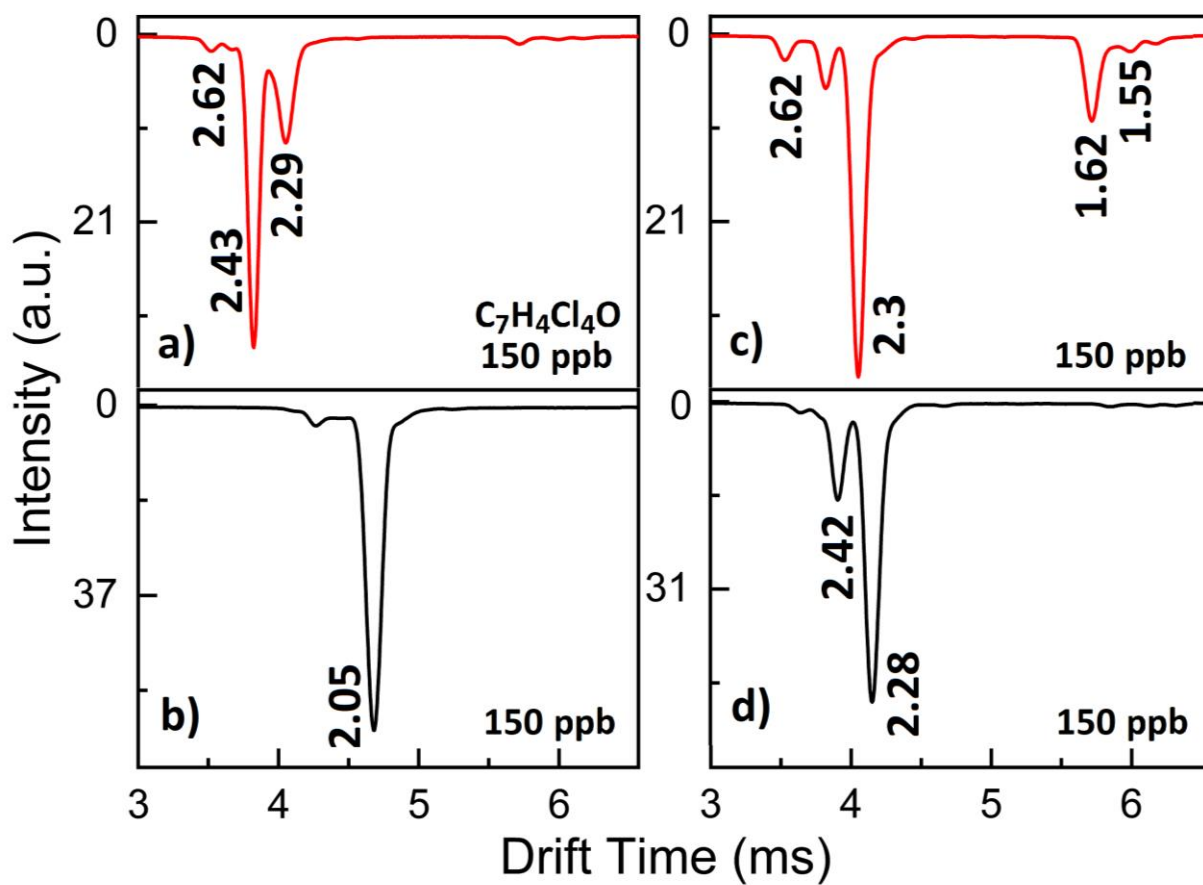


Figure S9. Negative ion mobility spectra of 2,3,5,6-Tetrachloroanisole (concentration 150 ppb) in the standard gas flow mode a) APFE, b) APCD ionisation sources and the reverse gas flow mode for c) APFE and d) APCD ionisation source.